

Table S1. Oligonucleotide primers used to obtain full length coding sequence of berry expressed LOXs

The sequences in bold were incorporated in order to facilitate directional cloning of a PCR fragment into pENTR™/TEV/D-TOPO® vector; the predicted translation initiation codon is underscored

Gene	Forward primer	Reverse primer
VvLOXA	5'- CACCA TGTTCAAGACTCAGGTCCA-3'	5'-TCAAATGGAGATACTGTATGGA-3'
VvLOXC	5'- CACCA TGATTCAATTGTTGGT-3'	5'-TTAGATGGAGACACTGTTGGAAATC-3'
VvLOXO	5'- CACCA TGGCAGTGGTAAAGAAATCAT-3'	5'-TCATATCGACACACTGTTGGAATCCC-3'

Table S2. Oligonucleotides used to amplify VvLOXA and VvLOXO for cloning into pENTR™ TEV/D-TOPO® vectors

Primer name	Sequence
LOXAFL_TOPO	5'-CACCTTCAAGACTCAGGTCCAC-3'
LOXA-TP_TOPO	5'-CACCGTTGGCTACGTCCCTGCCAACAT-3'
LOXATerm	5'-TCAAATGGAGATACTGTATGGAACT-3'
LOXOFL_TOPO	5'-CACCGCAGTGGTAAAGAAA-3'
LOXO-TP_TOPO	5'-CACCCCTGTTGGGCTGTGA-3'
LOXOTerm	5'-TCATATCGACACACTGTTGGAATCCC-3'

Table S3. Oligonucleotide primers used in real-time qPCR experiments

Gene	Forward primer	Reverse primer
<i>Actin</i>	5'-CTTGCATCCCTCAGCACCTT-3'	5'-TCCTGTGGACAATGGATGGA-3'
<i>GAPDH</i>	5'-ACTGCCCTGCTCCTCTTGCAGAAG-3'	5'-CCAGTGCTGCTAGGAATGATGTTGAATG-3'
<i>SAND</i>	5'-TGCCTGTTGATACATCTCCTCGCTCTG-3'	5'-TGGTGGTGAGAACTCCGAAGATACTACTG-3'
<i>EF1</i>	5'-GTGCGTCATAGTTTCTGCCCTCTCCTTG-3'	5'-CTCAACCAGTTATCTGCCACCGCCTATC-3'
<i>VvLOXA</i>	5'-GCAAATCAAAGGGACAACGCTGTATGG-3'	5'-TGCTTCCACTGCGGCTTCC-3'
<i>VvLOXC</i>	5'-TGGTCCAAGGAAGTCAGGGAAAGAG-3'	5'-TGGGCAGGTTGGGAGGTAGC-3'
<i>VvLOXD</i>	5'-ACCCACCAAATCGTCCCACACTATG-3'	5'-ACCTCTCGTTGTCTGTCCACTCTG-3'
<i>VvLOXO</i>	5'-TTCCACCCACTCGCCTGATG-3'	5'-GCACCGCACCTGTTCTCG-3'

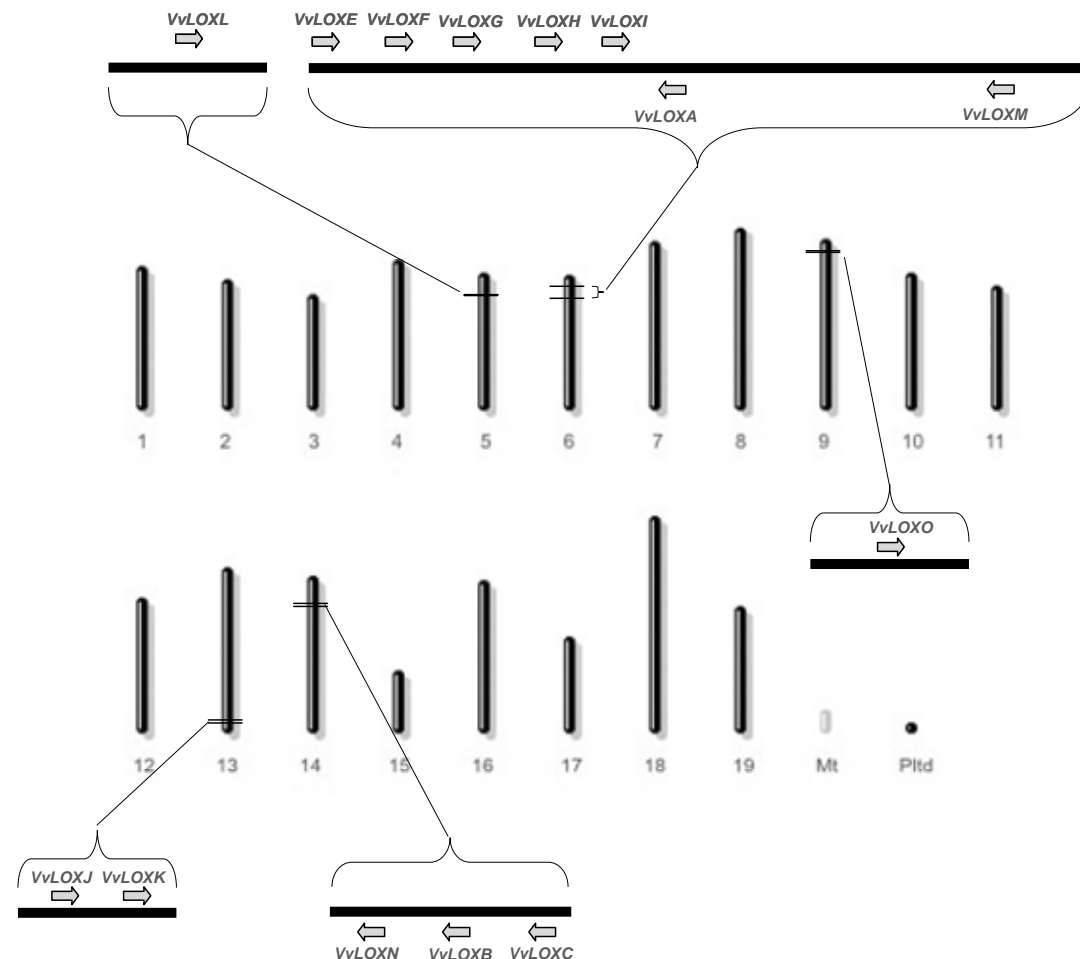


Fig. S1. Schematic representation of chromosomal location of the predicted grape LOX genes

Fourteen out of eighteen identified in the grape genome LOX genes were mapped with respect to the predicted grape chromosomes. The sequences of other four genes, *VvLOXD*, *VvLOXP*, *VvLOXR* and *VvLOXS* could not be linked to any of the existing chromosomes. Nineteen nuclear chromosomes, mitochondrial (Mt) and plastidial (Pltd) sub-genomes are schematically depicted. The arrows indicate 5' to 3' direction for the predicted coding sequences.

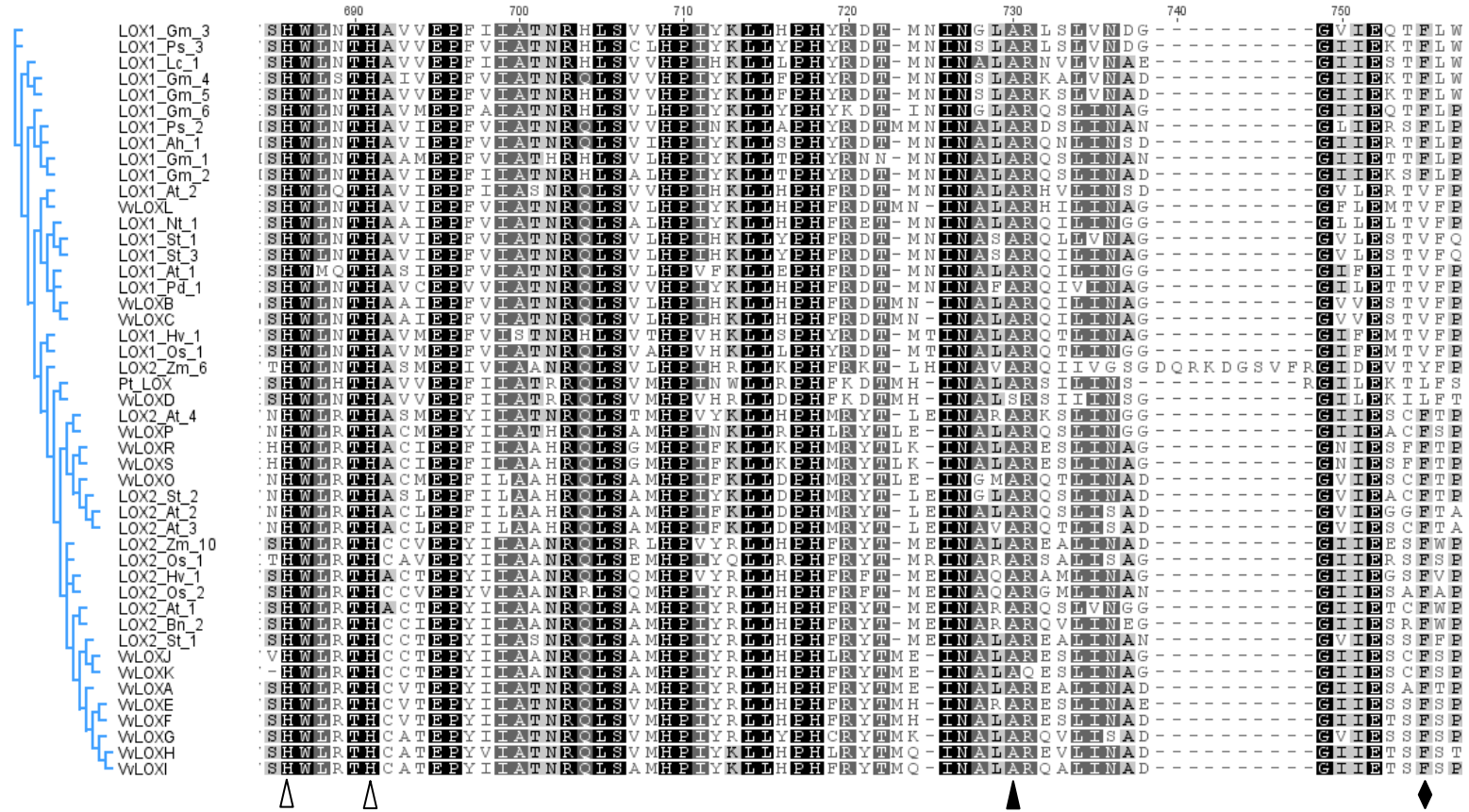


Fig. S2. Amino acid sequence alignment of the predicted Pinot noir LOXs and characterised plant LOXs

Only part of the alignment is shown containing important functional motifs and amino acid residues. The open triangles indicate amino acid residues involved in binding of catalytic atom of iron; black diamond and black triangle indicate amino acid residues involved in determining LOXs regiospecificity and stereospecificity respectively.

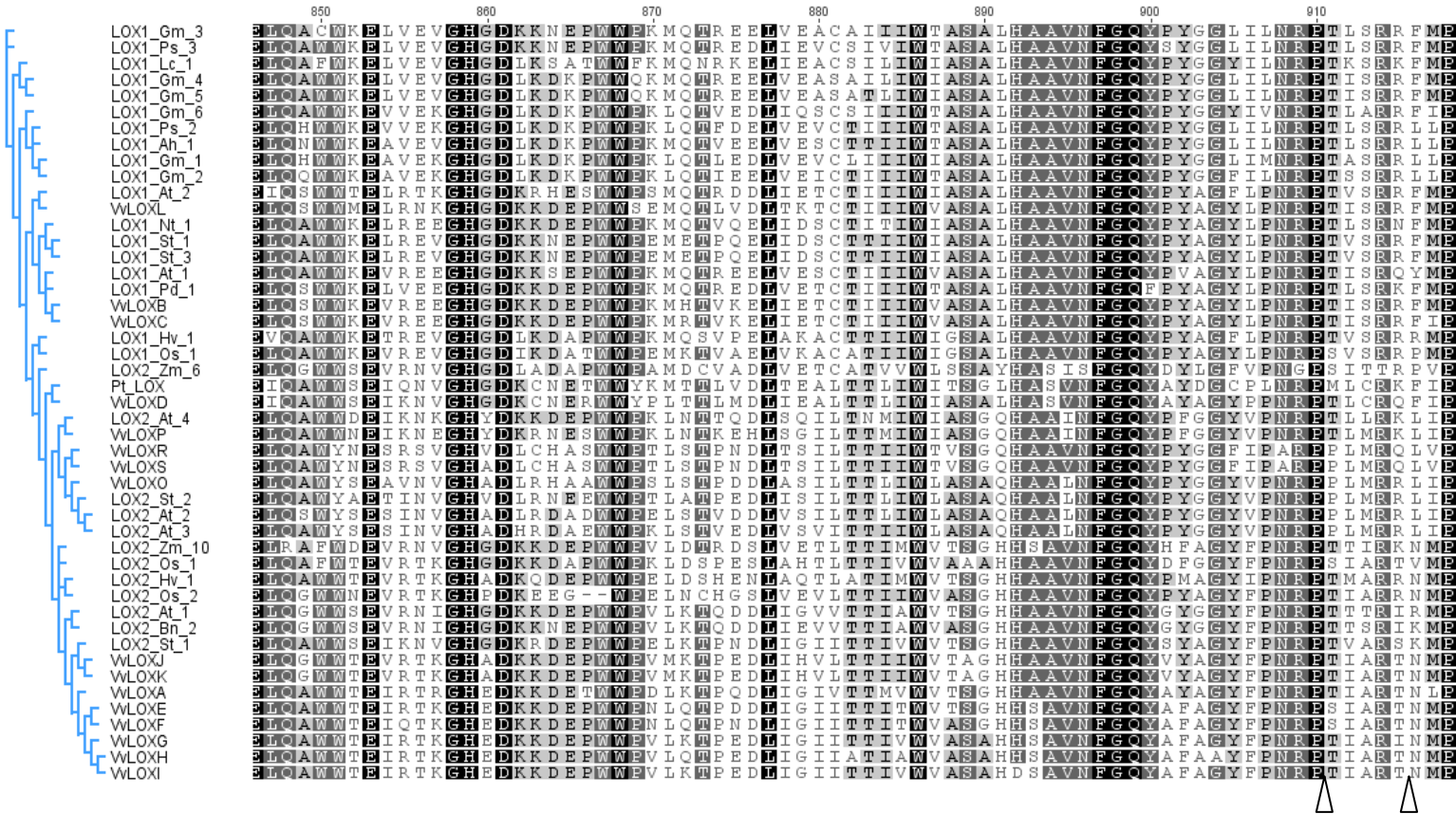


Fig. S2. (continued) Amino acid sequence alignment of the predicted Pinot noir LOXs and characterised plant LOXs

Only part of the alignment is shown containing important functional motifs and amino acid residues. The open triangles indicate amino acid residues involved in binding of catalytic atom of iron.

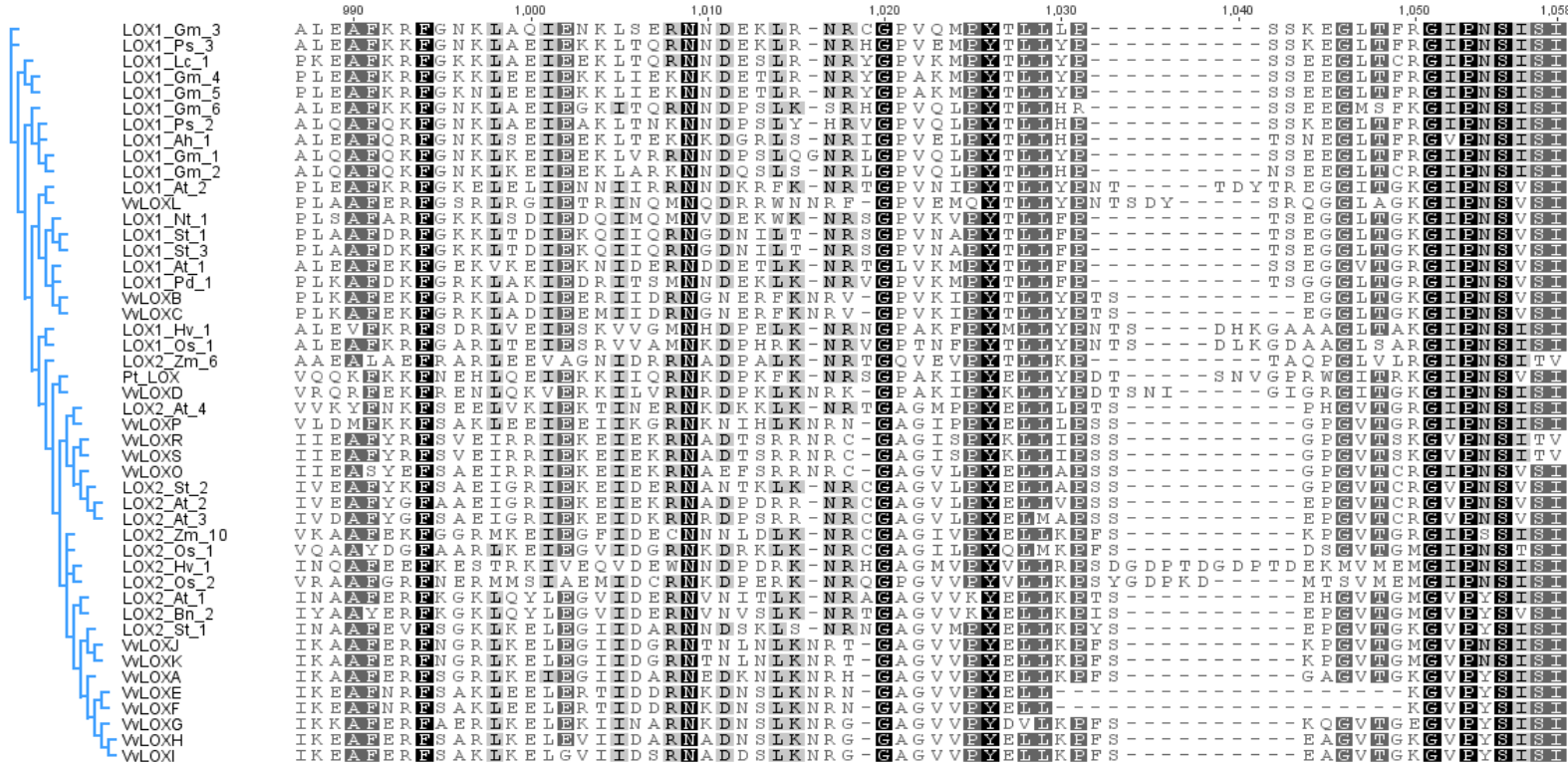


Fig. S2. (continued) Amino acid sequence alignment of the predicted Pinot noir LOXs and characterised plant LOXs

Only part of the alignment is shown containing important functional motifs and amino acid residues. The open triangle indicates amino acid residue involved in binding of catalytic atom of iron.

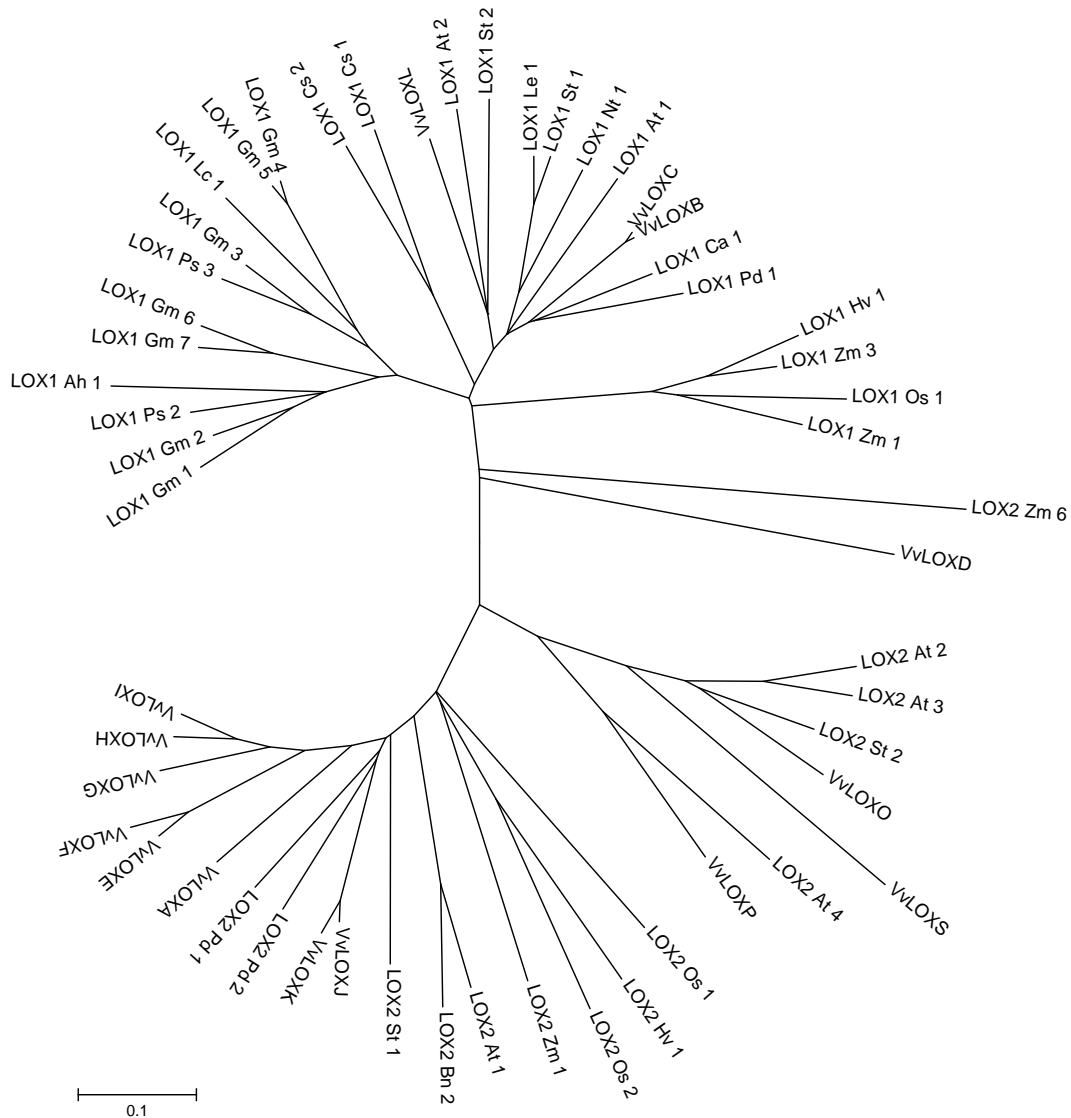
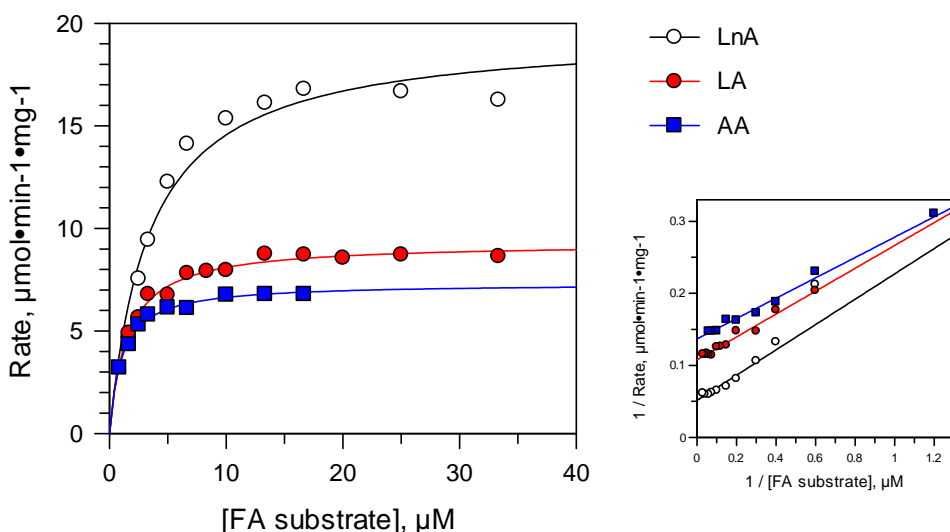


Fig. S3. Phylogenetic tree reconstructed based on the alignment of only the conserved LOX domains of grape and characterised LOX proteins

Conserved LOX domains of grape LOXs and characterised plant LOXs were aligned, and a tree was reconstructed to validate the tree obtained from a full-length LOX alignment (Fig. 2.). The evolutionary relationship was inferred using the Neighbour-Joining method (Saitou and Nei 1987). The bootstrap consensus tree inferred from 1000 replicates (Felsenstein 1985). Branches corresponding to partitions reproduced in less than 50% bootstrap replicates are collapsed. The tree is drawn to scale, with branch lengths in the same units as those of the evolutionary distances used to infer the phylogenetic tree. The evolutionary distances were computed using the Poisson correction method (Zuckerkandl, Pauling *et al.* 1965) and are in the units of the number of amino acid substitutions per site. All positions containing alignment gaps and missing data were eliminated only in pairwise sequence comparisons. Phylogenetic analyses were conducted in MEGA4 (Tamura, Dudley *et al.* 2007).. Tables 1 and 2 contain gene IDs and accession names for the LOXs used in the alignment.

Recombinant LOXA-TP Enzyme Kinetics Data

(A)



LnA:

Parameter	Value	Std. Error
Vmax	19.5626	0.9258
Km	3.4378	0.5789

LA:

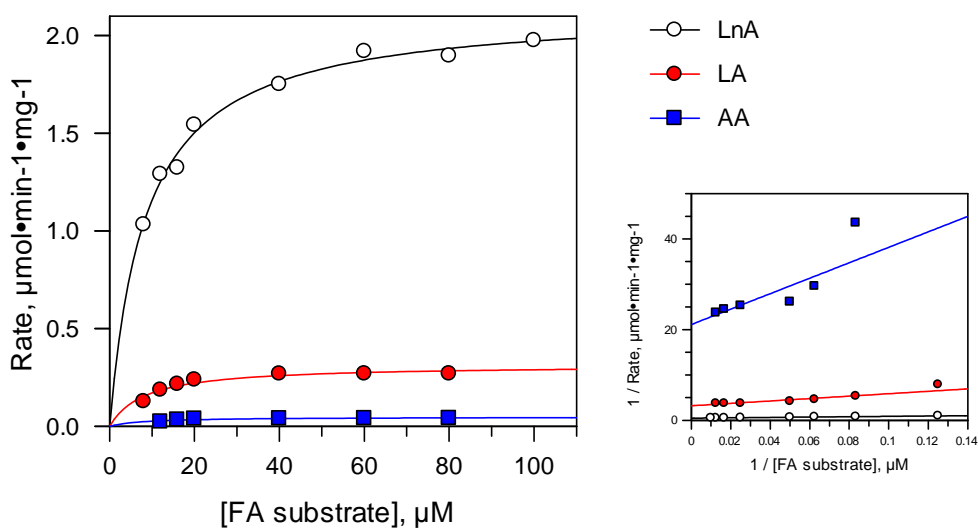
Parameter	Value	Std. Error
Vmax	9.2922	0.1494
Km	1.4747	0.1320

AA:

Parameter	Value	Std. Error
Vmax	7.3195	0.1135
Km	1.0336	0.0778

Recombinant LOXO-TP Enzyme Kinetics Data

(B)



LnA:

Parameter	Value	Std. Error
Vmax	2.1387	0.0381
Km	8.4818	0.6345

LA:

Parameter	Value	Std. Error
Vmax	0.3136	0.0175
Km	8.3591	1.8083

AA:

Parameter	Value	Std. Error
Vmax	0.0474	0.0042
Km	8.0747	3.1219

Fig. S4. The basic kinetic characteristics K_m and V_{\max} for recombinant LOXA-TP (a) and LOXO-TP (b) were determined by fitting the kinetic rate data with non-linear fit model described by Michaelis-Menten equation. Inserts on the right are Lineweaver-Burk plots.